Hall effect in potassium-hydrogen-graphite intercalation compounds and their conduction mechanism

Keisuke Nakazawa, Kazuya Suzuki, and Toshiaki Enoki
Department of Chemistry, Tokyo Institute of Technology, Ookayama, Meguro-ku, Tokyo 152, Japan

Yasuhiro Iye
Institute for Solid State Physics, University of Tokyo, Roppongi, Minato-ku, Tokyo 106, Japan

Ko Sugihara
College of Pharmacy, Nihon University, Narashinodai, Funabashi, Chiba 274, Japan

James T. Nicholls and Mildred S. Dresselhaus
Department of Physics, Massachusetts Institute of Technology, Cambridge, Massachusetts 02139
(Received 15 April 1992; revised manuscript received 22 July 1992)

The Hall effect and magnetoresistance were measured for stage-1 and -2 potassium-hydrogen-graphite ternary intercalation compounds (KH-GIC's) in the temperature range 1.4–250 K, in order to investigate their electronic structure and transport properties. The presence of two kinds of carriers was found: majority carriers in the graphitic π^* bands with electron character and minority hole carriers in the free-electron-like hydrogen 1*s* band. The hole carriers in the H 1*s* band are associated with the incomplete charge transfer to the hydrogen species. The Hall coefficient R_H and conductivity tensor σ_{xy} component exhibit large temperature dependences, which are considered to be due to the different in-plane scattering mechanisms for the two kinds of carriers. The hole carriers were found to have high mobilities, comparable to the mobilities of the graphitic π electrons. The scattering mechanism for the π^* bands can be explained in terms of an acoustic-phonon scattering process with small effective masses and a large deformation potential. On the other hand, that for the H 1*s* band is dominated by an acoustic-phonon scattering process, with a small deformation potential in the ionic K^+H^- intercalate layers below 80 K, in addition to a low-energy optical-phonon scattering, which is operative mainly at higher temperatures.

I. INTRODUCTION

The introduction of donors or acceptors into the galleries of the graphite host material forms graphite intercalation compounds (GIC's), which have a metallic character because of the injection of conduction carriers into the graphitic π bands. GIC's form a staged structure which is described in terms of the number of graphite layers between sequential intercalate layers. Recently, among GIC's, potassium-hydrogen-graphite ternary intercalation compounds (KH-GIC's) have been extensively investigated from the viewpoint of their novel electronic structure consisting of a two-dimensional metallic hydrogen system.[1–8] It is known that the stage-1 donor compound C_8K absorbs hydrogen at room temperatures through a chemisorption process,[9] and that it changes to a stage-2 ternary compound C_8KH_x, where the hydrogen concentration x is saturated at 0.67.[10] Isostructural analogs to the KH-GIC's obtained by chemisorption are also synthesized by the direct reaction of graphite with potassium hydride.[11] In this case, the compositions are described in terms of $C_{4s}KH_x$, where s expresses the stage number which takes on values of 1 or 2. The hydrogen concentration x ranges around 0.8, which is larger than the saturated concentration in the compound obtained by hydrogen chemisorption.

The hydrogen introduction in C_8K affects the electronic structure through the rearrangement of the charge distribution among the constituent atoms.[1] The hydrogen that is introduced behaves as an acceptor in C_8K so that the electrons in the potassium 4*s* band and in the graphitic π^* band are transferred to the hydrogen 1*s* band (H 1*s* band), since hydrogen has a strong electron affinity.[12] After charge transfer to hydrogen, there are no electrons in the potassium 4*s* band at the saturated hydrogen concentration.

It was found from x-ray[13] and neutron-scattering[14] measurements that KH-GIC's formed K^+-H^--K^+ triple ionic layer sandwiches in the intercalate gallery parallel to the stacking of the graphite layers. The in-plane structure of the intercalate is not fully understood, although several models have been proposed: $(2\times2)R(0°)$,[14,15] $(\sqrt{3}\times\sqrt{3})R(30°)$,[16] and $(2\sqrt{3}\times5)R(30°,0°)$ (Refs. 11,17, and 18) superstructures related to the graphite unit cell. Assuming the $(2\sqrt{3}\times5)R(30°,0°)$ superstructure which is most convincing from the recent neutron study,[18] the shortest interatomic distance of the hydrogen atoms is estimated to be 2.96 Å,[5] which is shorter than or about the same as the diameter of the H^- ions, 3.08 Å.[1] This means that the wave functions of adjacent hydrogen anions H^- can overlap with each other to form an extended electronic structure in the two-dimensional hydro-

gen lattice.[1,5]

In addition to the novel structure of the two-dimensional hydrogen lattice, an interesting hydrogen electronic state was recently demonstrated.[1-6] The presence of two kinds of carriers has been found through detailed studies of the ^{1}H-NMR,[2-5] thermoelectric power,[6] electronic specific heats,[19,20] and Shubnikov–de Haas measurements.[21] One has a large concentration of electron carriers in the graphitic π^* bands introduced by the charge transfer between graphite and the intercalate, and the other relates to hole carriers in the ionic intercalate layers whose concentration is so small that they can be neglected in comparison with the electron carriers to a first approximation. Based on experimental evidence,[1-6,19-21] it is thought that the hole carriers are associated with an incompletely filled H 1s band. This means that a novel two-dimensional metallic hydrogen state is present in the intercalate, taking into account the two-dimensional structure of the hydrogen lattice. The metallic hydrogen state demonstrated by the experiments is supported by the recent band calculations by Mizuno and Nakao.[7,8]

It is therefore important to obtain information on the transport properties of the carriers and on the electronic structure of these compounds in order to clarify the details of the novel metallic hydrogen state, in comparison with the hydrogen in transition metals which have been extensively studied as typical metal-hydrogen systems.[22] In this paper, we present results of measurements of the Hall effect and transverse magnetoresistance for stage-1 and stage-2 KH-GIC's, which give information on the mobilities of the electron and hole carriers, and we discuss the conduction mechanism of both types of carriers.

II. EXPERIMENT

KH-GIC samples were synthesized by means of the direct intercalation method[11] with potassium hydride and highly oriented pyrolytic graphite (Union Carbide HOPG). Potassium hydride and HOPG were heat treated in a vacuum-sealed Pyrex glass tube. Stage-1 KH-GIC samples were obtained under these conditions in the temperature range 380 °C–430 °C for one to two weeks, and stage-2 KH-GIC in the range 210 °C–250 °C for two to four months. The products were reddish-violet for the stage-1 KH-GIC, and dark blue for stage-2 KH-GIC. They were characterized by means of (001) x-ray-diffraction patterns. The c-axis repeat distances I_c were 8.54 and 11.90 Å for stage-1 and -2 KH-GIC's, respectively. The x-ray-diffraction patterns suggested that stage-1 samples contained a trace of the stage-2 KH-GIC (less than 5%), while no second phases were found in stage-2 samples.

The Hall resistance and transverse magnetoresistance were measured for a magnetic field parallel to the c axis. The measurements were performed under the conditions of (1) up to magnetic fields of 23 T at liquid-helium temperatures (4.2 K) and (2) up to 9 T in the temperature range 1.4–250 K. Typical sample dimensions were $4\times8\times0.3$ mm^3. Six copper or gold wires with diameters of 50 or 100 μm were cemented by use of silver cement on the samples as electrodes. The Hall voltage (the direction is $\perp$ current and $\perp$ field) and transverse voltage (the direction is $\parallel$ current and $\perp$ field) were measured by use of a Keithley 181 nanovoltmeter using direct currents of 10 or 20 mA parallel to the c plane. The measurements up to 23 T were performed by use of a Bitter-type magnet. A fast Fourier transform was performed to analyze the observed Shubnikov–de Haas oscillations.

III. EXPERIMENTAL RESULTS

Figures 1 and 2 show the magnetoresistance results $\Delta\rho/\rho_0$ and the Hall resistivity ρ_{xy} for stage-1 and -2 KH-GIC's (sample indices are labeled by No. n) as a function of magnetic field B up to 23 T at different temperatures, where ρ_0 is the resistivity at zero magnetic field and $\Delta\rho(T,B)=\rho(T,B)-\rho(T,0)$. For both stages, the magnetoresistance decreases with increasing temperature, as shown in Fig. 2. Since $\Delta\rho/\rho_0$ is generally zero on the basis of the simple one-carrier model with a closed orbit,[23] the presence of temperature and magnetic-field dependences in $\Delta\rho/\rho_0$ suggests that the band structure cannot be expressed in terms of a simple one-carrier model. Shubnikov–de Haas (SdH) oscillations are observed

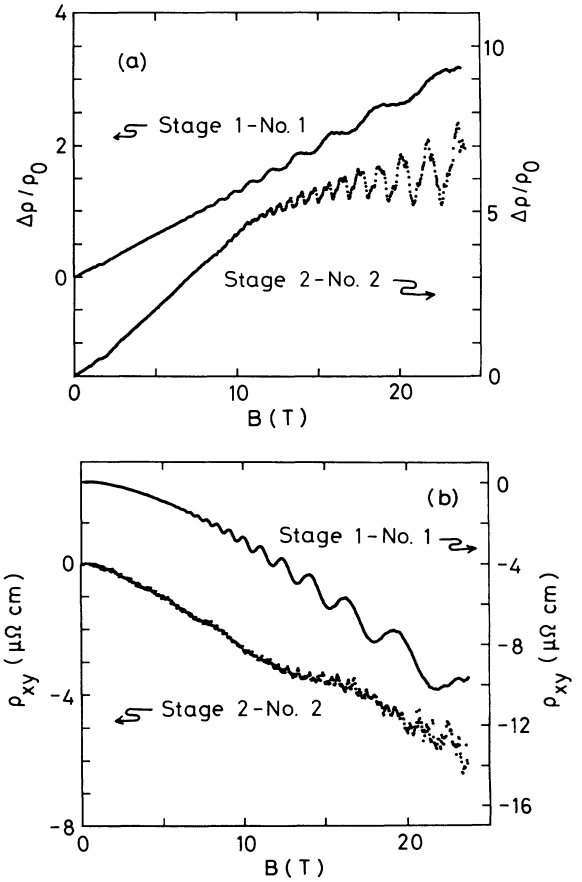

FIG. 1. Magnetic-field dependence of (a) the magnetoresistance $\Delta\rho/\rho_0$ normalized by the zero-field resistivity ρ_0, and (b) the Hall resistivity ρ_{xy} for stage-1–No. 1 and stage-2–No. 2 KH-GIC samples at 4.2 K up to 23 T.

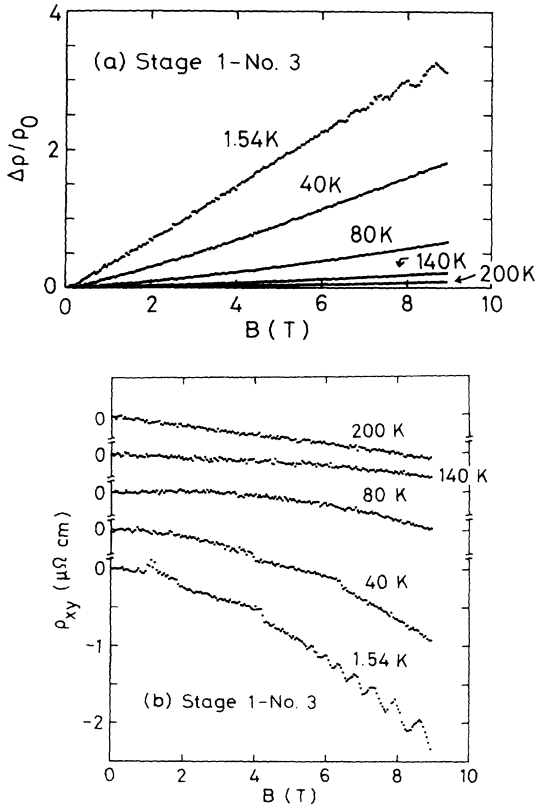

FIG. 2. Temperature dependence of (a) the magnetoresistance $\Delta\rho/\rho_0$ and (b) the Hall resistivity ρ_{xy} for a stage-1–No. 3 KH-GIC sample up to 9 T. The observed jumps in the 1.54-K (at 1 and 4 T) and 40-K (at 4 and 6 T) curve in ρ_{xy} are caused by changes in instrumental conditions.

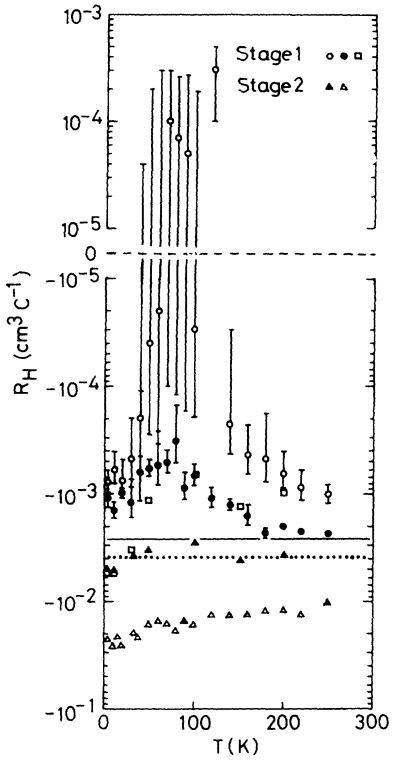

FIG. 3. Temperature dependence of the Hall coefficient R_H estimated at 1 T. ○, ●, and □ denote R_H for stage-1 KH-GIC samples (sample indices Nos. 3, 4, and 5, respectively), and △ and ▲ for stage-2 samples (Nos. 6 and 7, respectively). The solid and dotted lines denote the estimated R_H from the optical studies (Refs. 24 and 25) for stage 1 ($R_H=-2.74\times10^{-3}$ cm^3C^{-1}) and stage 2 ($R_H=-3.88\times10^{-3}$ cm^3C^{-1}) KH-GIC's, respectively, on the basis of a one-carrier model.

for both compounds above 6 T below 10 K, as shown in Figs. 1 and 2. In the stage-2 KH-GIC, a low-frequency SdH oscillation is observed below 10 K whose oscillation vanishes above 2.5 T, as shown in Fig. 1.

The Hall coefficient R_H is defined in terms of the Hall resistivity ρ_{xy} as $R_H=\rho_{xy}/B$.[23] In the case of a one-carrier model for metallic states, no magnetic-field dependence is expected for R_H, so that ρ_{xy} should be proportional to B. The observed field dependences of ρ_{xy} for both stage compounds do not obey a simple linear function of B as shown in Figs. 1 and 2, and suggest that the one-carrier model is not able to explain the transport properties of KH-GIC's. As shown in Fig. 3, we estimate R_H as a function of temperature at $B=1$ T where the linear magnetic-field dependence $\rho_{xy}\propto B$ is realized. The estimated R_H has a sample dependence, and it is believed that the sample dependence comes partly from experimental errors in the determination of the distances between electrodes, and partly from impurity levels that vary from one sample to another. The negative signs of the observed R_H over the whole temperature range indicate that the predominant carriers are electrons. [One of the stage-1 samples (No. 3) had small positive values of the Hall coefficient in the temperature range from 40 to 120 K, as shown in Fig. 3.] Whereas R_H tends to become less negative with increasing temperature in the stage-2 KH-GIC, the R_H measurements show a large temperature dependence with the maximum value at about 80 K in the stage-1 KH-GIC (where the absolute value is a minimum). Optical reflectance experiments[24,25] suggest that the majority carriers are associated with the graphitic π electrons which have electron character. If we assume that the R_H data are explained in terms of only one kind of π-electron carrier in this system, R_H must be independent of temperature, and inversely proportional to carrier concentration. In Fig. 3, we also show (with solid and dotted lines) the estimated R_H on the basis of a one-carrier model ($R_H=1/ne$) with one kind of electron carrier on the graphitic π^* bands whose concentration n is calculated from the optical experiments.[24,25] The temperature dependence of the observed R_H within experimental error significantly deviates from the estimated R_H. Thus the nonlinear magnetic-field dependence in ρ_{xy} and the strong temperature dependence in R_H (with a change in sign to positive values around 80 K for the stage-1–No. 3 sample) in the experiments suggest the coexistence of electron and hole carriers, and this interpretation is also consistent with thermoelectric power experiments.[6] The contribution of the hole carriers to R_H in the stage-2 KH-GIC seems to be smaller than that in the stage-1 KH-GIC, since the experimental results in the stage-2 KH-GIC show a weaker temperature dependence

of R_H and more negative R_H values.

We convert the measured resistivities to conductivity tensors which depend on the applied magnetic field to estimate the carrier concentrations and mobilities. The conductivity tensors σ_{xx} and σ_{xy} are related to resistivity tensors ρ_{xx} and ρ_{xy} according to[26]

$$\sigma_{xx}=\frac{\rho_{xx}}{\rho_{xx}^2+\rho_{xy}^2}\ , \tag{1}$$

$$\sigma_{xy}=\frac{\rho_{xy}}{\rho_{xx}^2+\rho_{xy}^2}\ . \tag{2}$$

Using Eqs. (1) and (2), σ_{xx} and σ_{xy} for the stage-1–No. 1 and stage-2–No. 2 KH-GIC samples are calculated as a function of magnetic field up to 23 T at 4.2 K and the results are shown in Figs. 4 and 5. In the stage-1–No. 1 KH-GIC sample, a contribution from hole carriers with positive signs in σ_{xy} is clearly observed below 1 T. In systems with multiple carriers, σ_{xx} and σ_{xy} are expressed as a function of magnetic field by the following equations:

$$\sigma_{xx}=\sum_i \frac{n_i|e_i|\mu_i}{1+(\mu_i B)^2}\ , \tag{3}$$

$$\sigma_{xy}=\sum_i \frac{n_i e_i \mu_i^2 B}{1+(\mu_i B)^2}\ . \tag{4}$$

Here n_i are the carrier concentrations and μ_i are the mobilities for the ith carriers. Since the hole and electron carriers contribute to Eq. (4) with opposite signs, the magnetic-field dependence is more evident in σ_{xy} than in σ_{xx} for a system with coexisting electron and hole carriers. Therefore, we gave a large weight to the σ_{xy} data in the least-squares fitting of the experimental results with the magnetic-field dependence expressed in Eq. (4).

In the stage-1 KH-GIC samples, a two-carrier model was employed to fit the experimental data for σ_{xy}, where the fitting parameters n_e and μ_e were used for the electrons and n_h and μ_h for the holes. The best-fitting curves for the stage-1–No. 1 KH-GIC sample as a function of magnetic field up to 23 T at 4.2 K are shown in Fig. 4 with the experimental results. The concentration of electron carriers n_e is estimated to be on the order of 10^{20} cm^{-3} and the mobility μ_e about 1000 $cm^2 V^{-1} s^{-1}$. The concentration of hole carriers n_h is estimated to be on the order of 10^{19} cm^{-3} and the mobility μ_h is comparatively large, about 7000 $cm^2 V^{-1} s^{-1}$ at 4.2 K. Therefore, n_e is 10 to 100 times larger than n_h.

We also calculate σ_{xx} as a function of magnetic field as shown in Fig. 4, using Eq. (3) with the best-fitting parameters obtained for σ_{xy}. The magnitude of the predicted σ_{xx} is about one-half as small as the observed σ_{xx}, although we have qualitative agreement in the magnetic-field dependence between the predicted and observed σ_{xx}. This discrepancy in σ_{xx} is attributed to experimental errors coming from the determination of the distance between electrodes.

Using Eq. (4), the estimated mobilities from the σ_{xy} data at 4.2 K in the stage-1 samples are summarized in Table I, which shows the sample dependence in the mag-

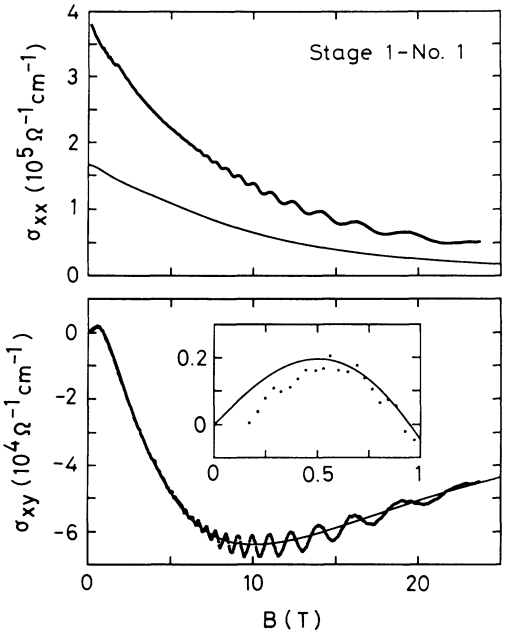

FIG. 4. Field dependence of σ_{xx} and σ_{xy} for a stage-1–No. 1 KH-GIC sample at 4.2 K up to 23 T. The inset in the σ_{xy} plot denotes the details of the positive contribution below 1 T. The solid lines indicate the best-fitting curves on the basis of the two-carrier model (one electron and one hole): $n_e=8.1\times10^{20}$ cm^{-3}, $n_h=2.6\times10^{19}$ cm^{-3}, $\mu_e=1050$ $cm^2 V^{-1} s^{-1}$, and $\mu_h=7000$ $cm^2 V^{-1} s^{-1}$.

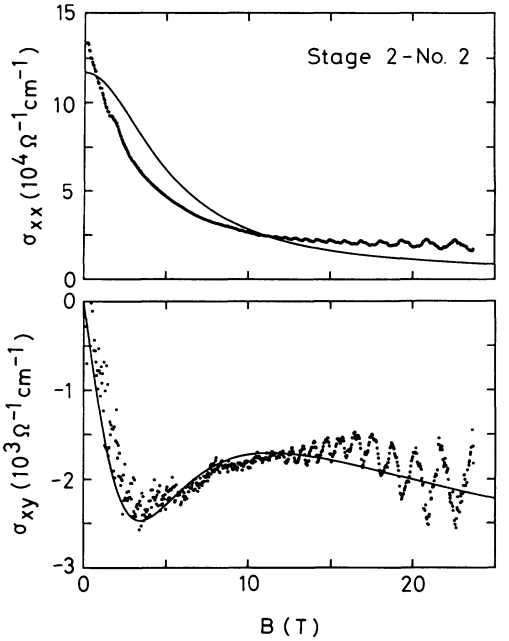

FIG. 5. Field dependence of σ_{xx} and σ_{xy} for a stage-2–No. 2 KH-GIC sample up to 23 T. The solid lines indicate the best-fitting curves on the basis of the three-carrier model (two electrons and one hole): $n_{e,1}=1.8\times10^{20}$ cm^{-3}, $n_{e,2}=1.6\times10^{20}$ cm^{-3}, $n_h=1.78\times10^{20}$ cm^{-3}, $\mu_{e,1}=2000$ $cm^2 V^{-1} s^{-1}$, $\mu_{e,2}=200$ $cm^2 V^{-1} s^{-1}$, and $\mu_h=1900$ $cm^2 V^{-1} s^{-1}$.

TABLE I. Estimated mobilities ($cm^2 V^{-1} s^{-1}$) from σ_{xy} curve fittings at 4.2 K. The subscripts e denote the electron carriers and h the hole carriers (see the text). The lines for samples 4, 6, and 7 mean that reasonable mobility values could not be calculated due to large ambiguity in the estimation.

Stage 1 KH-GIC			Stage 2 KH-GIC			
sample	μ_e	μ_h	sample	$\mu_{e,1}$	$\mu_{e,2}$	μ_h
1	1050	7000	2	2000	200	1900
3	3000	4000	6	—	—	—
4	—	—	7	—	—	—
5	782	781				

nitude of μ_e and μ_h. The sample dependence is attributed to a difference in the strength of the impurity scattering in the samples, as mentioned above in discussing the sample dependence of R_H.

The magnetic-field dependence of σ_{xy} up to 9 T was obtained at several temperatures in the stage-1–No. 3 KH-GIC sample, as shown in Fig. 6, and the results exhibit a large temperature dependence. There is some small discrepancy in the behavior of σ_{xy} between Figs. 4 and 6 at liquid-helium temperatures, which is thought to be due to a difference in impurity concentrations in the samples, as mentioned above. It is probable that the sample shown in Fig. 4 (sample No. 1) is purer than that in Fig. 6 (sample No. 3) because of the presence of clearer SdH oscillations. In Fig. 6, we also show the fitting curves for each of the three temperatures after the least-squares fitting. Basically the behavior of the observed σ_{xy} is electron dominant over the whole temperature range (1.54, 80, and 140 K). However, in the field dependence at 80 K, a small contribution from hole carriers is seen at low magnetic fields below 3 T.

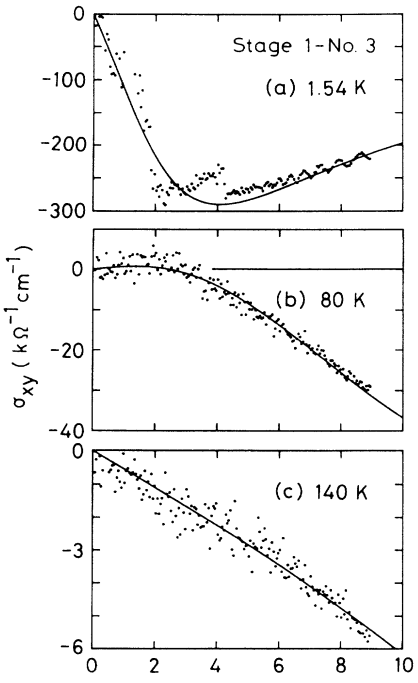

FIG. 6. Temperature dependence of σ_{xy} for a stage-1–No. 3 KH-GIC sample. The solid lines indicate the best-fitting curves on the basis of the two-carrier model with constant carrier concentrations, $n_e = 2.2 \times 10^{21}$ cm^{-3} and $n_h = 8.0 \times 10^{20}$ cm^{-3}. (a) $\mu_e = 3000$ $cm^2 V^{-1} s^{-1}$, $\mu_h = 4000$ $cm^2 V^{-1} s^{-1}$ at 1.54 K, (b) $\mu_e = 669$ $cm^2 V^{-1} s^{-1}$, $\mu_h = 1136$ $cm^2 V^{-1} s^{-1}$ at 80 K, and (c) $\mu_e = 255$ $cm^2 V^{-1} s^{-1}$, $\mu_h = 369$ $cm^2 V^{-1} s^{-1}$ at 140 K. The observed jumps between 2 and 4 T at 1.54 K are caused by instrumental conditions.

We next show the conductivity tensors for the stage-2 KH-GIC. σ_{xy} must go to zero at extremely high field, as demonstrated in Eq. (4). Then, in the σ_{xy} vs B curve for the stage-2–No. 2 KH-GIC sample shown in Fig. 5, two minima with negative signs should be found around 3 T and at a field higher than 25 T. Moreover, it seems that a small concentration of hole carriers might also be present, and might also contribute to increasing the experimental value of σ_{xx} in the σ_{xx} vs B curve. Therefore, the fitting parameters of σ_{xy} are obtained by means of a three-carrier model (two electrons and one hole) in Fig. 5. The electron carrier concentrations $n_{e,1}$ and $n_{e,2}$, where the subscripts denote band indices, are estimated to be about the same, about 10^{20} cm^{-3}. The electron mobility $\mu_{e,1}$, whose contribution strongly influences the minimum in σ_{xy} around 3 T in Fig. 5, is estimated to be around 200 $cm^2 V^{-1} s^{-1}$. The electron mobility $\mu_{e,2}$, which strongly affects the decrease in σ_{xy} at high fields, is about 200 $cm^2 V^{-1} s^{-1}$, so that the mobilities for these two kinds of electron carriers differ by about one order of magnitude. The concentration n_h and mobility μ_h for the hole carriers are found to be on the order of 10^{20} cm^{-3} and 2000 $cm^2 V^{-1} s^{-1}$, respectively. The estimated mobilities are summarized in Table I. The observed two kinds of electron carriers are reasonable due to the two π bands in stage 2. The fitting parameters of the experimental σ_{xy} are in comparatively good agreement with σ_{xx}, as shown in Fig. 5. However, the estimated electron and hole concentrations are too small and large, respectively, in comparison with the estimated concentrations by the ^{1}H-NMR (Ref. 3) and optical measurements.[24,25] Then, the estimated carrier concentrations from Fig. 5 are not accurate, perhaps due to experimental errors and the influence of the zone-folded π bands.[21]

As shown in Figs. 1 and 2, in the traces for the magnetoresistance and the Hall resistivity, SdH oscillations are observed above 6 T in the temperature range below 10 K for both stage-1 and -2 KH-GIC's. The SdH frequency F_i and its corresponding Fermi-surface cross-sectional area S_i (Ref. 27) are listed in Table II for the stage-1–No. 1 and stage-2–No. 2 samples in comparison with previous results by Enoki *et al.*[21] It is likely that the lack of high-frequency oscillations in the stage-1–No. 1 sample in comparison with the results of Ref. 21 may be caused by inhomogeneities of the samples. In the stage-2–No. 2 KH-GIC sample, a fundamental oscillation is observed at 2527 T (F_ζ) in addition to the oscillations observed in the previous paper.[21] A SdH oscillation F_α with a frequency of 2.10 T is also observed below 2.5 T for the stage-2 KH-GIC.

We analyze the π-band Fermi surfaces of the stage-2

TABLE II. Observed SdH frequencies F and corresponding Fermi-surface cross-sectional areas S of stage-1–No. 1 and stage-2–No. 2 KH-GIC samples.

	Stage 1 KH-GIC (No. 1)				Stage 2 KH-GIC (No. 2)		
	F (T)	S (Å^{-2})	F (T)[a]		F (T)	S (Å^{-2})	F (T)[a]
α			30	α	2.10	0.000 201	
β	107	0.0102	106	β			41
γ			647	γ	264	0.0252	283
δ			4000	δ	791	0.0755	763
				ε	1410	0.135	1525
				ζ	2527	0.241	

[a]Reference 21.

KH-GIC on the basis of the SdH effect. The two-dimensional π-band model[28] can be used for the analysis of the electronic structure since the π electrons are well separated from the holes in the hydrogen band by the ionized potassium layers. We neglect the $F_\zeta=2527$ T frequency since this SdH oscillation is less reproducible if we compare the present results with the results in Ref. 21 and the oscillation gives a larger Fermi energy than that estimated from the optical studies.[24,25] Thus, if we assign the SdH frequencies $F_\delta=791$ T (corresponding to the Fermi wave number $k_F^+=0.155$ Å^{-1}) and $F_\varepsilon=1410$ T (corresponding to the Fermi wave number $k_F^-=0.207$ Å^{-1}) to be the cylindrical Fermi surfaces for the upper and the lower graphitic π^* band, respectively,[21] the intralayer and interlayer resonance integrals are estimated to be $\gamma_0=2.9$ eV and $\gamma_1=0.32$ eV, respectively, using the Fermi energy $E_F=1.13$ eV obtained by the optical studies.[24,25] These values for γ_0 and γ_1 are in good agreement with the reported values for graphite: $\gamma_0=3.12$ eV and $\gamma_1=0.377$ eV.[29] The charge transfer per carbon atom f_C (Refs. 28 and 30) is also estimated to be $f_C=0.028$. For the composition of $C_8KH_{0.8}$, the charge transfer of hydrogen f_H is estimated to be $f_H=-0.97$, taking into account the charge neutrality among C, K, and H, since the K 4s orbital is completely empty.[7,8] The finding that f_H is nearly -1 is consistent with the results of the optical experiments.[24,25]

Here, we show the modification of the Fermi surfaces by the in-plane zone-folding effects, on the basis of the SdH oscillations. It has been believed that the in-plane superstructure of the intercalate for KH-GIC's forms a $(2\sqrt{3}\times5)R(30°,0°)$ lattice by recent x-ray and neutron experiments,[11,17,18] whose Brillouin zones are illustrated in Fig. 7 with the original Brillouin zone of graphite. The low-frequency oscillation γ observed in the stage-2 KH-GIC just fits a Fermi surface modified by the in-plane zone-folding effects for the upper π^* bands (+) when adjacent original Fermi surfaces overlap with each other in the folded Brillouin zone. On the other hand, $(2\times2)R(0°)$ and $(\sqrt{3}\times\sqrt{3})R(30°)$ superstructures, which were suggested in early works on the in-plane structure of KH-GIC's,[14–16] cannot make the in-plane zone-folding effects because the lower π^* bands k_F^- (generally $>k_F^+$) are smaller than one-half of the distance between the centers of the nearest-neighborhood Fermi surfaces, 0.851 and 0.983 Å^{-1} for the 2×2 and $\sqrt{3}\times\sqrt{3}$ superstructures, respectively. Therefore, the experimental fact suggests that the $2\sqrt{3}\times5$ superstructure forms the in-plane zone-folded Fermi surfaces in KH-GIC's.

The origin of the frequency F_α has two possibilities: one from residue graphite regions and the other from the Fermi surfaces modified by the zone-folding effects. Pristine graphite has three oscillations (0.34, 4.52, and 6.14 T) (Ref. 31) which are different from the observed frequency $F_\alpha=2.10$ T. Moreover, the observed oscillation F_α has the identical frequency for all the stage-2 samples investigated in the present measurements, even though the quality varies depending on samples. Therefore, the oscillation is considered to be associated with the electronic structure modified in the folded Brillouin zone.

IV. DISCUSSION

We discuss the transport properties of the carriers in KH-GIC's. The optical reflectance[24,25] and SdH studies[21] suggested that the majority electron carriers originate from the graphitic π^* bands in KH-GIC's, while ^{1}H-NMR studies[2–5] revealed the presence of minority hole carriers associated with the incompletely filled H 1s band. The ratio of the local density of states for hydrogen sites $N_H(E_F)$ to the total density of states $N(E_F)$ is estimated to be $N_H(E_F)/N(E_F)\sim0.01$ for stage-2 $C_8KH_{0.55}$.[3] The stage-1 KH-GIC has a larger $N_H(E_F)$ than the stage 2.[5] The Seebeck coefficient indicates a positive contribution

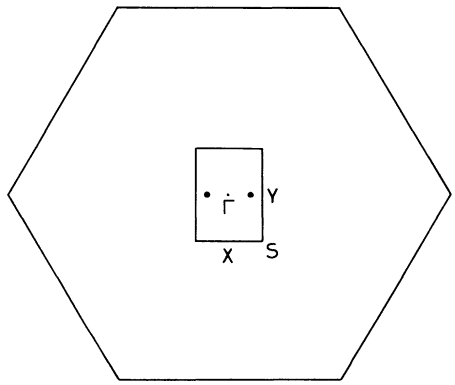

FIG. 7. The first Brillouin zone of a $(2\sqrt{3}\times5)R(30°,0°)$ superlattice which is illustrated with respect to the graphitic hexagonal Brillouin zone. The length of a side in the graphitic Brillouin zone is 1.703 Å^{-1}. The small full circles indicate the centers of the Fermi surfaces in the superlattice.

below 30 K for both stage-1 and stage-2 KH-GIC's which is attributed to the diffusion term of the hole carriers.[6,32] The experimental findings of the coexistence of majority electron carriers and minority hole carriers are supported by the theoretical studies done by Mizuno and Nakao.[7,8] They demonstrated the presence of a H 1*s* hole band with free-electron character which is superposed on the graphitic π^* bands, giving rise to the majority electron carriers.

The present results on the Hall effect and magnetoresistance are consistent with the electronic structures demonstrated by these experiments and theories. σ_{xy} in Figs. 5 and 6 prove that there is one kind of electron carrier and one kind of hole carrier for the stage-1 KH-GIC sample, and two kinds of electron carriers and one kind of hole carrier for the stage-2 KH-GIC sample. As mentioned above, the small Fermi surfaces generated by the zone-folding effects for the graphitic π^* bands can give small concentrations of additional carriers, some of which will be of hole character. However, the contributions to the transport of the carriers belonging to these small Fermi surfaces are effective only at low temperatures, since the thermal energy will work to restore the original π bands if the thermal energy exceeds the energy gaps generated by the zone folding. This means that, at liquid-helium temperatures, the observed positive values of σ_{xy} in the stage-1–No. 1 sample (see Fig. 4) can include contributions from the small π^*-band Fermi surfaces generated by the zone-folding effects, while the hole carriers observed between 40 and 120 K in the stage-1–No. 3 sample (see Fig. 6) are attributed to the H 1*s* band with two-dimensional free-electron character. This is consistent with the experimental findings that the positive contribution to σ_{xy} has a larger sample dependence at lower temperatures than those at higher temperatures above 40 K.

We discuss the behavior of the carriers on the basis of a two-carrier model with the graphitic π electrons and holes in the H 1*s* band for the stage-1 KH-GIC. Figure 8

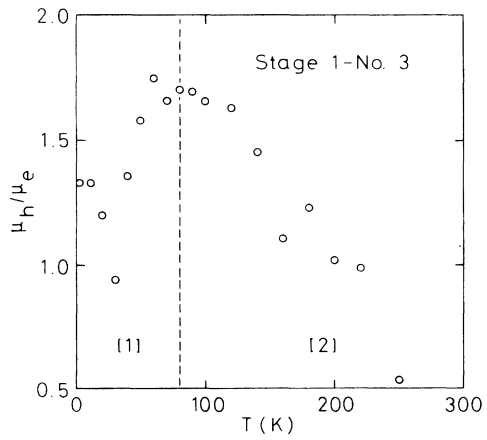

FIG. 8. Temperature dependence of the mobility ratio μ_h/μ_e estimated from the best fitting σ_{xy} for a stage-1–No. 3 KH-GIC sample. The dashed line at 80 K indicates the boundary between the low-temperature region (1) and the high-temperature region (2) where the ratio μ_h/μ_e has different temperature dependences from each other.

shows the temperature dependence of the mobility ratio μ_h/μ_e for the stage-1–No. 3 KH-GIC sample estimated from the least-squares fitting of σ_{xy}. In the intermediate temperature range around 80 K, the estimated values of μ_h/μ_e are more accurate than those at lower and higher temperatures, since the magnetic-field dependence is well characterized in terms of electron and hole carriers in this temperature range. The results show that μ_h/μ_e increases with increasing temperature, reaches a maximum value at about 80 K, and decreases with further increase in temperature. From a comparison between Figs. 3 and 8, we can see that the contribution of the hole carriers to σ_{xy} around 80 K is related to the maximum in the R_H vs T curve. This means that, in the intermediate temperature range, the mobilities of the holes are more enhanced than those of the electrons in comparison with the lower and higher temperature range, even though the whole transport process is dominated by electron carriers over the whole temperature range. The experimental fact that μ_h/μ_e depends on temperature suggests that the conduction processes of the two kinds of carriers are different from each other. The large temperature dependence of the mobility ratio μ_h/μ_e is classified into two regions: (1) μ_h/μ_e increases with increasing temperature for $T \leq 80$ K. (2) μ_h/μ_e decreases with temperature for $T \geq 80$ K.

At liquid-helium temperatures in Region 1, the impurity scattering process is predominant. It is assumed that the graphitic π electrons are scattered by lattice defects associated with boundaries of the graphene sheets, while the hole carriers in the H 1*s* band are predominantly scattered by ionic impurities and vacancies in the intercalate layers. The strength of the impurity scattering depends on the quality of the samples, as the mobility ratio μ_h/μ_e has a large sample dependence. Moreover, the contribution of the hole carriers in the H 1*s* band and that generated from the zone-folding effects for the π^* band both modify the observed conductivities in the low-temperature region. Then, the intrinsic contribution of the H 1*s* hole carriers is ambiguous at low temperatures, as we can see the difference in the behaviors of σ_{xy} between Figs. 4 and 6. Therefore, we cannot make any clear interpretation for the behavior of the hole mobility in this low-temperature range.

Above 10 K (Region 1), the acoustic-phonon scattering process becomes predominant for both electron and hole carriers. The graphitic π electrons in GIC's have large mobilities on the order of 10^3 cm^2 V^{-1} s^{-1} at intermediate temperatures,[33] since the graphitic π-bands have small effective masses ($\sim 0.1 m_e$). The behavior of the mobilities in ordinary GIC's is analogous to the electron carriers in the π^* bands of KH-GIC's which also have small effective masses (~ 0.01–$0.2 m_e$).[7,8,21] Here, we discuss the reason why the hole carriers in the H 1*s* band have large mobilities as well as the mobilities of the graphitic π-electron carriers in intermediate temperatures (Region 1, see Fig. 8). In KH-GIC's, while the effective masses of the graphitic π electrons m_C, where subscript C denotes the graphitic π^* band, are small as discussed above, those of the holes in the H 1*s* band m_H, where subscript H denotes the H 1*s* band, are about $3m_e$ with

two-dimensional free-electron character, as estimated from the band calculations by Mizuno and Nakao.[7,8] Therefore, the large difference in the effective masses between the two carriers indicates a higher mobility for the graphite π electrons than the holes in the H 1s band. The disagreement with the experimental results can be explained in terms of the difference in deformation potentials for the electron-phonon coupling related to the acoustic phonons between the π electrons in the graphite layers and the holes in the K^+H^- ionic intercalate layers. The relaxation times τ_{ac} for the acoustic-phonon scattering process in the two-dimensional metallic state are expressed by the following equation:[34]

$$\frac{1}{\tau_{ac}} \simeq \frac{D^2 k_B T}{2\pi I_c d \hbar v^2} \times \int_0^{\infty} \int_0^{\pi} dq\, d\theta\, q \{\delta[E(\mathbf{k}+\mathbf{q})-E(\mathbf{k})] + \delta[E(\mathbf{k}-\mathbf{q})-E(\mathbf{k})]\} , \quad (5)$$

where D denotes the deformation potential, d the crystal density, v the sound velocity, and $\mathbf{q}$ and $\mathbf{k}$ are the in-plane wave vectors. In stage-1 GIC's, the energy dispersions of the graphitic π band[28] and the H 1s band are given by the following equations:

$$E = p_0 k , \quad (6)$$

$$E = \frac{\hbar^2 k^2}{2m_H} , \quad (7)$$

respectively, where $p_0 = 3\gamma_0 b/2$ where b ($=1.42$ Å) is the in-plane C-C distance. Using Eqs. (5)–(7), the ratio of the relaxation times between the graphitic π^* band $\tau_{ac,C}$ and the H 1s band $\tau_{ac,H}$ is obtained as follows:

$$\frac{\tau_{ac,H}}{\tau_{ac,C}} = \frac{d_H}{d_C} \left[\frac{v_H D_C}{v_C D_H} \right]^2 \frac{\hbar^2 k_C}{m_H p_0} . \quad (8)$$

In Eq. (8), we put $2d_H \sim d_C$ and $k_C = 0.247$ Å^{-1} [by use of $\gamma_0 = 2.9$ eV and $E_C = 1.53$ eV (Refs. 24 and 25)] for the stage-1 KH-GIC according to the discussion in Ref. 32. (The factor of 2 in Eq. (5) in Ref. 32 should be deleted.) The sound velocities might be $6v_H \sim v_C$ because the Debye temperatures of potassium hydride and graphite in-plane are 409 (Ref. 35) and 2480 K,[36] respectively. The deformation potential D_C for the graphitic layers is large with a magnitude of 16 eV.[34] The Fermi energy for the H 1s band is small, ranging around 0.6 eV from the band calculations.[7,8] Thus the deformation potential D_H related to the acoustic phonons for the holes in the intercalate layer is considered to be 0.4 eV by use of $D = 2E_F/3$. Using Eq. (8) with the above estimated parameters and effective masses, the mobilities of the electrons in the graphitic π^* band and the holes in the H 1s band associated with the acoustic-phonon scattering processes are found to be $\mu_H \sim \mu_C$ or $\mu_H < \mu_C$. This estimation is qualitatively in good agreement with the present experimental results ($\mu_h \sim \mu_e$). Thus the large mobility of the hole carriers in the H 1s band is caused by the small deformation potential which counteracts the effect of the heavy effective mass in the transport processes. In Region 1, the increasing μ_h/μ_e with increasing temperature up to 80 K is considered to be caused by the different energy dispersion relations between the two kinds of bands, as described in Eqs. (6) and (7). The temperature dependence of these carrier relaxation times is not known exactly. However, the difference in the band dispersions will give different temperature dependences in the carrier relaxation times for the two carriers.

Above 80 K (Region 2), the contribution of the hole carriers rapidly decreases, as shown in Figs. 3 and 8. In the phonon states of KH-GIC's, there coexist acoustic and low-energy optic phonons. The experimental results of the lattice specific heats give the Einstein temperature $\theta_E \sim 58$ K for optic phonons related to the K^+H^- ionic intercalate in the stage-2 KH-GIC,[19,20] while pristine graphite has no low-energy optic phonons.[37] Since the optic phonons contribute to scattering processes at high temperatures, the decreasing μ_h/μ_e above 80 K means that the optic phonons excited at high temperatures above θ_E scatter the hole carriers in the intercalate consisting of the K^+-H^--K^+ ionic lattice. However, the π electrons in the graphitic layers are not much affected by the excitations of the optic phonons in the intercalate layers. For the hole carriers, the relaxation time associated with optic phonons is expressed as

$$\tau_{op,H} = C \left[\exp\left(\frac{\theta_E}{T} \right) - 1 \right] , \quad (9)$$

where C is a constant dependent on the optic-phonon frequency.[38] Equation (9) suggests that the relaxation time related to the optic-phonon scattering process rapidly decreases at high temperatures for the hole carriers. The trend of the temperature dependence expressed in Eq. (9) is consistent with the behavior of μ_h/μ_e, as demonstrated in Fig. 8.

V. CONCLUSION

The Hall effect and magnetoresistance for stage-1 and -2 KH-GIC's were investigated up to 23 T between 1.4 and 250 K to examine the electronic structure and the transport mechanisms of KH-GIC's with the coexistence of carriers in the graphitic π bands and the hydrogen 1s band.

In the stage-1 KH-GIC, R_H and σ_{xy} have large temperature dependences which are interpreted to reflect the coexistence of majority electron carriers from the graphitic π^* bands with minority holes from the H 1s band. The experimental results are analyzed on the basis of a two-carrier model. The hole carriers were found to have high mobilities (on the order of 10^3 cm^2 V^{-1} s^{-1}) comparable to the mobilities of the graphite π electrons. The mobility ratio μ_h/μ_e has a large temperature dependence indicating different transport mechanisms for these two types of carriers. The behavior of the estimated mobility ratio μ_h/μ_e is classified into two temperature regions, depending on the scattering mechanism of the hole carriers. The high mobility of the hole carriers in the H 1s band is explained in terms of a small deformation potential for acoustic phonon scattering below 80 K, and is affected by

the optic phonons generated in the K^+H^- ionic intercalate layers above 80 K.

The temperature dependence of R_H in the stage-2 KH-GIC is smaller than that of the stage-1 KH-GIC. Accordingly, the R_H behavior indicates that the holes in the stage-2 KH-GIC influence the transport properties less than those in the stage-1 KH-GIC.

ACKNOWLEDGMENTS

We thank Dr. A. W. Moore of Union Carbide for his generous gift of HOPG, and are grateful to Professor G. Dresselhaus of Massachusetts Institute of Technology, Professor W. R. Datars of McMaster University, and Professor Y. Yosida of Iwaki Meisei University for fruitful discussion. This work was supported partly by the Grant-in-Aid for Scientific Research No. 02453009 from the Ministry of Education, Science and Culture, Japan and partly by the Mitsubishi Science Foundation. The work done at MIT was supported by NSF Grant No. DMR 88-19896. We acknowledge use of the high-field magnets at the Francis Bitter National Magnet Laboratory, supported by the National Science Foundation.

[1]T. Enoki, S. Miyajima, M. Sano, and H. Inokuchi, J. Mater. Res. **5**, 435 (1990).

[2]K. Nomura, T. Saito, K. Kume, and H. Suematsu, Solid State Commun. **63**, 1059 (1987).

[3]S. Miyajima, T. Chiba, T. Enoki, H. Inokuchi, and M. Sano, Phys. Rev. B **37**, 3246 (1988).

[4]T. Saito, K. Nomura, K. Mizoguchi, K. Mizuno, K. Kume, and H. Suematsu, J. Phys. Soc. Jpn. **58**, 269 (1989).

[5]S. Miyajima, M. Kabasawa, T. Chiba, T. Enoki, Y. Maruyama, and H. Inokuchi, Phys. Rev. Lett. **64**, 319 (1990).

[6]T. Enoki, K. Imaeda, H. Inokuchi, and M. Sano, Phys. Rev. B **35**, 9399 (1987).

[7]S. Mizuno and K. Nakao, J. Phys. Soc. Jpn. **58**, 3679 (1989).

[8]S. Mizuno and K. Nakao, Phys. Rev. B **41**, 4938 (1990).

[9]D. Saehr and A. Hérold, Bull. Soc. Chim. Fr., 3130 (1965).

[10]M. Colin and A. Hérold, Bull. Soc. Chim, Fr., 1982 (1971).

[11]D. Guérard, C. Takoudjou, and F. Rousseaux, Synth. Met. **7**, 43 (1983).

[12]From de Haas–van Alphen results, it was recently demonstrated that C_8K indicates complete charge transfer from the potassium band. However, some of this charge is associated with interlayer states. We argue that the electrons going to hydrogen-derived states come from the interlayer states [G. Wang, W. R. Datars, and P. K. Ummat, Phys. Rev. B **44**, 8294 (1991)].

[13]G. Furdin, P. Lagrange, A. Hérold, and C. Zeller, C. R. Acad. Sci. (Paris) C **282**, 563 (1976).

[14]T. Trewern, R. K. Thomas, G. Naylor, and W. White, J. Chem. Soc. Faraday Trans. 1 **78**, 2369 (1982).

[15]J. Conard, H. Estrade-Szwarckopf, P. Lauginie, M. El Makrini, P. Lagrange, and D. Guérard, Synth. Met. **2**, 261 (1980).

[16]L. Salamanca-Riba, N.-C. Yeh, M. S. Dresselhaus, M. Endo, and T. Enoki, J. Mater. Res. **1**, 177 (1986).

[17]D. Guérard, N. E. Elalem, C. Takoudjou, and F. Rousseaux, Synth. Met. **12**, 195 (1985).

[18]W. A. Kamitakahara, G. Doll, and P. C. Eklund, in *Extended Abstracts,* Proceedings of Symposium K, 1986 Fall Meeting of the Materials Research Society, edited by M. S. Dresselhaus, G. Dresselhaus, and S. A. Solin (Materials Research Society, Boston, 1986), p. 69.

[19]T. Enoki, M. Sano, and H. Inokuchi, Synth. Met. **12**, 207 (1985).

[20]T. Enoki, M. Sano, and H. Inokuchi, Phys. Rev. B **32**, 2497 (1985).

[21]T. Enoki, N.-C. Yeh, S.-T. Chen, and M. S. Dresselhaus, Phys. Rev. B **33**, 1292 (1986).

[22]*Hydrogen in Metals I & II,* edited by G. Alefeld and J. Völkl, Topics in Applied Physics Vols. 28 and 29 (Springer-Verlag, Berlin, 1978).

[23]A. H. Wilson, *The Theory of Metals,* 2nd ed. (Cambridge University Press, London, 1953), pp. 208–231.

[24]G. L. Doll, M. H. Yang, and P. C. Eklund, Phys. Rev. B **35**, 9790 (1987).

[25]G. L. Doll and P. C. Eklund, J. Mater. Res. **2**, 638 (1987).

[26]D. E. Soule, Phys. Rev. **112**, 698 (1958).

[27]*Electrons at the Fermi Surface,* edited by M. Springford (Cambridge University Press, London, 1980).

[28]J. Blinowski, N. Hy Hau, C. Rigaux, J. P. Vieren, R. Le Toullec, G. Furdin, A. Hérold, and J. Melin, J. Phys. (Paris) **41**, 47 (1980); Eq. (17) in this paper is misprinted (see Ref. 30).

[29]M. S. Dresselhaus, G. Dresselhaus, and J. E. Fischer, Phys. Rev. B **15**, 3180 (1977).

[30]J. M. Zhang, P. C. Eklund, Y. B. Fan, and S. A. Solin, Phys. Rev. B **38**, 10 878 (1988).

[31]N. B. Brandt, A. S. Kotosonov, and M. V. Semenov, Zh. Eksp. Teor. Fiz. **79**, 937 (1980) [Sov. Phys. JETP **52**, 476 (1980)].

[32]K. Sugihara, T. Enoki, and K. Nakazawa, Mater. Sci. Forum **91-93**, 439 (1992).

[33]M. S. Dresselhaus and G. Dresselhaus, Adv. Phys. **30**, 139 (1981).

[34]K. Sugihara, Phys. Rev. B **28**, 2157 (1983).

[35]B. N. Oshcherin, Zh. Fiz. Khim. **50**, 2994 (1976).

[36]K. Komatsu, J. Phys. Soc. Jpn. **10**, 346 (1955).

[37]M. G. Alexander, D. P. Goshorn, and D. G. Onn, Phys. Rev. B **22**, 4535 (1980).

[38]*Solid State Physics,* edited by R. Kubo and T. Nagamiya (McGraw-Hill, New York, 1969), pp. 157–162.